第 48 卷 第 7 期/2021 年 4 月/中国激光 研究论文

中国激光

基于波长调制吸收光谱的燃烧流场二维重建

王兴平[1,2]，彭冬[1]，李佳胜[1]，金熠[3*]，翟超[3]

[1]中国科学技术大学工程科学学院，安徽 合肥 230027；

[2]中国科学院安徽光学精密机械研究所，安徽 合肥 230027；

[3]中国科学技术大学工程与材料科学实验中心，安徽 合肥 230027

摘要 可调谐二极管激光吸收光谱(TDLAS)技术是进行燃烧流场关键参数测量的有效有段。采用近红外水蒸汽的两条吸收线(7168.44 cm^{-1} 与 7185.60 cm^{-1})，分别利用直接吸收法与波长调制法对不同噪声干扰下的高斯峰流场进行了温度重建的数值仿真。将波长调制法和直接吸收法的二维重建结果进行对比，结果显示基于波长调制法的二维重建有更强的抗噪声能力。以 McKenna 平面燃烧炉产生的甲烷-空气预混火焰为测量对象，进行了二维温度重建。实验结果显示基于直接吸收法和波长调制法的二维重建的最大偏差分别为 8.5%和 5.9%，均方相对误差分别为 0.0469 和 0.0268。弱吸收下基于波长调制法的二维重建技术显示了更好的重建效果。

关键词 激光技术；光谱学；波长调制；二维重建；燃烧诊断

中图分类号 O433 **文献标志码** A **doi**：10.3788/CJL202148.0711002

1 引 言

燃烧流场关键参数的测量能有效评估燃烧效率、控制污染排放和提高能源利用率[1]，可调谐二极管激光吸收光谱(TDLAS)技术因其具有高精度、非接触测量、低成本等优点，适用于燃烧流场中温度[2]、体积分数[3]、速度[4]及压力[5]等关键参数的测量[2,6-7]。TDLAS 技术结合电子计算机断层扫描技术，还可实现二维层析成像[8-9]甚至三维层析成像[10]，这进一步扩展了该技术的发展前景。

二维重建技术可追溯至 20 世纪 80 年代，Emmerman 等[11]使用直接吸收光谱(DAS)技术对甲烷射流的气体浓度进行了二维重建，验证了该方法的可行性，随后各国学者开展了广泛研究。Gorenflo 等[12]研究了射线数目不足导致的欠定方程组求解问题，并尝试用 Abel 变换解决该问题。Ma 等[13]研究了使用高光谱吸收光谱同时重建温度和浓度的方法，结果表明该方法显著地降低了射线数目要求。Ling 等[14]在现有的代数迭代重建算法基础上，提出了计算效率更高的自适应代数迭代重建(MAART)算法。Terzija 等[15]优化了原有的射线布置方式，提出了重建精度更高的不规则射线布置方式。随着研究人员对激光器的发展与重建算法的深入研究，基于 DAS 的二维重建技术开始应用于工程实践中，如美国空军实验室和 NASA 等单位在高超音速国际飞行研究实验(HIFiRE)中使用了该技术[16]。虽然 DAS 技术表现出高灵敏、高精度、低硬件成本等诸多优势，但该方法难以适用于弱吸收等低信噪比的情况。在 DAS 技术基础上发展而来的波长调制光谱学(WMS)方法可以显著提高弱吸收条件下的信噪比，并可提高吸收光谱技术的检测精度与检测极限。斯坦福大学的 Hanson 课题组提出的免标定波长调制光谱技术[17](CF-WMS)为使用较为广泛的 WMS 方法之一。为了减小燃烧流场等恶劣环境对重建精度的影响，Silver 等[18]将 WMS 方法引入二维重建中，并对湍流火焰进行了重建研究。此后，Guha 等[19]利用数值仿真的方法分析了基于 DAS 和 WMS 的两种不同测量方法对重建精度的影响；Zhao 等[20]将基于 WMS 的二维重建方法应用于风洞出口的温度与水含量二维分布测量；Cai 等[21]利

收稿日期：2020-08-24；**修回日期**：2020-09-05；**录用日期**：2020-11-02

基金项目：国家自然科学基金(11202204)、基础性军工科研院所稳定支持项目(DD2090009001)

*E-mail：yjin@ustc.edu.cn

用 CF-WMS 方法结合模拟退火算法实现了恶劣环境下的温度与浓度的二维重建；彭冬[22]将 CF-WMS 方法与代数迭代重建算法相结合，通过数值仿真分析了不同噪声强度及不同温度下的重建效果。目前工程应用中多以一维测量为主，张步强等[23]利用 WMS 方法建立了精确的温度测量模型，屈东胜等[24]利用 WMS 方法对超燃直连台隔离段和扩张段进行了多参数测量，姚德龙等[25]对固体火箭燃烧羽流进行了气流速度测量。总的来说，基于 WMS 的二维重建技术已显示出在弱吸收恶劣燃烧流场测量中的潜力，但其诸多特点仍需进一步的研究和验证。

本文首先介绍了基于 WMS 的二维温度重建的原理，其次通过数值仿真分析了不同噪声影响下基于 DAS、WMS 的二维温度重建效果差异，结果表明二维重建中，基于 WMS 的二维重建技术对噪声的抑制能力明显优于基于 DAS 的二维重建技术。最后使用 McKenna 平焰炉产生的燃烧流场作为测量对象，并围绕该平焰炉搭建了二维温度测量实验系统。对甲烷-空气预混火焰进行了基于 DAS 与 WMS 的二维温度重建，分析了基于这两种方法的二维温度重建结果。

2 基本原理和吸收谱线选择

2.1 波长调制吸收光谱

当频率为 $\nu(\mathrm{cm}^{-1})$ 的激光穿过光程为 $L(\mathrm{cm})$、压强为 $P(\mathrm{atm})$、吸收组分体积分数为 X、温度为 $T(K)$ 的流场后，激光入射光强 I_0 和透射光强 I_t 之间满足 Beer-Lambert 定律：

$$\tau(\nu)=\frac{I_t}{I_0}=\exp\left\{-\int_0^L P(x)X(x)S[T(x)]\varphi(\nu)\mathrm{d}x\right\}=\exp[-\alpha(\nu)], \tag{1}$$

式中：$\tau(\nu)$ 为激光透射系数；$\alpha(\nu)$ 为吸收率；$\varphi(\nu)$ 为吸收谱线线型函数；S 为线强度。经过调制深度为 a 的余弦信号的调制后，将激光透射系数按余弦级数展开为

$$\tau(\nu)=\sum_{k=0}^{\infty}H_k\cos(k\theta), \tag{2}$$

式中：$H_k=\frac{1}{n\pi}\int_{-\pi}^{\pi}\tau(\nu')\cos(k\theta)\mathrm{d}\theta$，当 $k=0$ 时，$n=2$，其他情况下 $n=1$，$\nu'=\nu+a\cos\theta$。在弱吸收条件下[$\alpha(\nu)<0.05$]，$\tau(\nu)\approx1-\alpha(\nu)$，$H_k$ 可简化为

$$H_k=-\frac{1}{n\pi}\int_0^L\int_{-\pi}^{\pi}PXS(T)\varphi(\nu')\cos(k\theta)\mathrm{d}\theta\mathrm{d}x。 \tag{3}$$

中心频率处，透射信号的二次谐波幅值 $2f$ 与一次谐波幅值 $1f$ 的比值为[1]

$$S_{2f/1f}=\frac{1}{i_0\pi}\int_0^L\int_{-\pi}^{\pi}PXS(T)\varphi(\nu')\cos(2\theta)\mathrm{d}\theta\mathrm{d}x, \tag{4}$$

式中：i_0 为激光光强线性调制系数。通过法布里-珀罗标准具可以测得光强线性调制系数与调制深度。

2.2 二维重建

待测流场被均匀划分化为 $N\times N$ 个网格。假设单个网格内流场分布均匀，即单个网格内温度、压力、体积分数均匀分布，因此单个网格内的吸收系数随光程呈线性变化，即谐波信号也随光程呈线性变化。根据(4)式，可以将穿过待测流场射线的谐波系数 H_k 看作路径上各网格之和，则 $S_{2f/1f}$ 为

$$S_{2f/1f}=\frac{1}{i_0\pi}\sum_{j=1}^{J}P_jX_jl_jS(T_j)\int_{-\pi}^{\pi}\varphi(\nu')\cos(2\theta)\mathrm{d}\theta=\sum_{j=1}^{J}h_{2,j}l_j, \tag{5}$$

其中

$$h_{2,j}=\frac{1}{i_0\pi}P_jX_jS(T_j)\int_{-\pi}^{\pi}\varphi(\nu')\cos(2\theta)\mathrm{d}\theta, \tag{6}$$

式中：l_j 为射线穿过第 j 个网格的光程；P_j 为第 j 个网格的压强；X_j 为第 j 个网格的待测气体的体积分数；T_j 为第 j 个网格的温度；$h_{2,j}$ 表示第 j 个网格的吸收系数。

利用 MAART 算法[14]，对交叉布置的射线的 $S_{2f/1f}$ 组成的线性方程组进行计算，可求得各网格的 h_2（任意一个网格的吸收系数）。

二维温度场重建的计算流程图如图 1 所示，首先获得射线经过各网格的光程 L、网格数 J、流场压强 P。利用锁相放大技术，获得各透射光强 I_t 的中心频率处的 $S_{2f/1f}$。通过 MAART 算法求解(5)式，得到各网格的吸收系数 h_2。通过测量得到双线比，即 $(h_{2,\upsilon_1,j}/h_{2,\upsilon_2,j})_m$，对比仿真数据库 $(h_{2,\upsilon_1,j}/h_{2,\upsilon_2,j})_s$，对体积分数 X 进行迭代计算，得到流场温度 T。

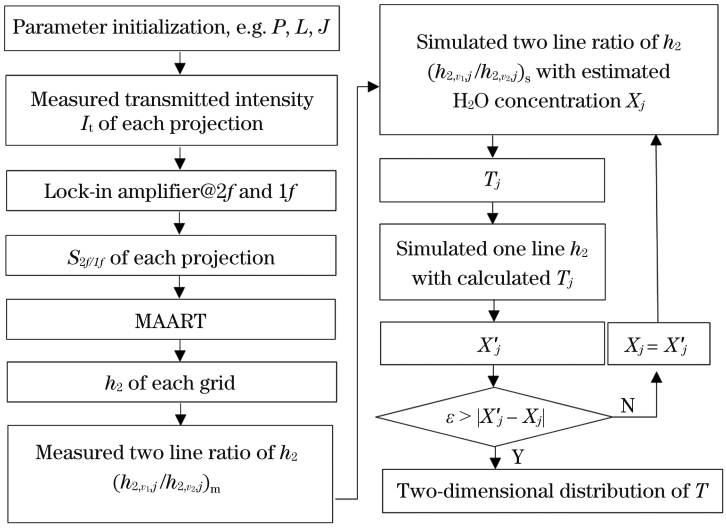

图 1　温度场重建计算流程图

Fig. 1　Flow chart of reconstruction of temperature field

2.3　吸收谱线选择

对于燃烧流场，水汽是常见的产物之一，且水汽在近红外处有较多可选的孤立吸收峰，本文选择一组近红外的两条水汽吸收线，即 7185.60 cm^{-1} 及 7168.44 cm^{-1} 作为吸收谱线，进行弱吸收下燃烧流场的温度重建研究。所选谱线的光谱参数来源于 HITRAN 2016 数据库，见表 1。

表 1　水蒸汽测温吸收谱线参数

Table 1　Spectral line parameters of temperature measurement for H_2O

Center frequency ν_0 /cm^{-1}	Absorption line intensity S /(cm^{-2} · atm^{-1})	Energy at low state E'' /cm^{-1}
7185.60	7.91×10^{-22}	1045.06
7168.44	1.17×10^{-20}	173.37

3　数值仿真

3.1　数值仿真模型

采用 10 cm×10 cm 的矩形流场作为燃烧流场的仿真模型。矩形流场被均匀划分为 10×10 个网格，并假设单个网格内的流场均匀分布，即单个网格内温度、压力、体积分数均匀分布；射线分布为 10×10 的正交分布。如图 2 所示，矩形流场的温度场分布符合高斯函数分布，即矩形流场中间处温度最高，为 1050 K；从中心到边缘矩形流场的温度逐渐降低，最低温度为 200 K；矩形流场的水汽分压 X_{H_2O} 分布均匀，PX_{H_2O}=10.1325 Pa。通过仿真可得两条吸收谱线的中心频率处的最大吸收率分别为 α_{1395}=0.02<0.05 和 α_{1392}=0.0008<0.05，满足弱吸收条件。

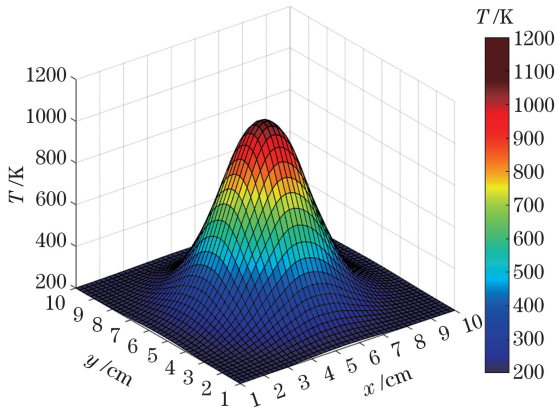

图 2　初始温度分布

Fig. 2　Initial temperature distribution

3.2　仿真结果

通过最大偏差 E_m 及均方相对误差 D_e 衡量重建误差，最大偏差为重建结果与原始结果的最大差值，均方相对误差为重建相对偏差的均方根值。E_m 和 D_e 可分别表示为

$$\begin{cases} D_e = \sqrt{\dfrac{1}{J}\sum_{j=1}^{J}\left[\dfrac{T_j^{rec}-T_j^{orig}}{\max(T_j^{orig})-\min(T_j^{orig})}\right]^2} \\ E_m = \max(|T^{rec}-T^{orig}|) \end{cases}, \quad (7)$$

式中：T_j^{rec} 为第 j 个网格的重建温度；T_j^{orig} 为第 j 个网格的初始温度；T^{rec} 为温度重建结果；T^{orig} 为初始温度。

为了对比波长调制法与直接吸收法在二维重建中对噪声的抑制能力，需要对模拟的燃烧流场添加噪声。本文通过文献[26]中方法产生噪声强度 I_{RIN} 分别为 −160 dB/Hz、−150 dB/Hz、−140 dB/Hz 的透射光光强信号，并基于这种噪声分布的光强信

号，分别利用 DAS 与 WMS 对模拟的燃烧流场进行温度重建。

表 2 及图 3 显示了两种重建方法在不同噪声强度影响下的模拟流场的温度重建结果。在无噪声条件下，基于 WMS 和 DAS 进行重建得到的最大偏差与均方相对误差较为一致，分别为 0.0186、40.3 K 与 0.0192、42.5 K。随着噪声强度的增加，基于 DAS 的重建技术的误差逐渐增大，而基于 WMS 的重建技术的误差变化不明显。在噪声强度为 −140 dB/Hz 的条件下，基于 WMS、DAS 的重建技术的最大偏差与均方相对误差存在较大的区别，分别为 0.0206、49.8 K 与 0.0795、353.6 K。

表 2　不同噪声强度下基于 WMS 与 DAS 得到的二维温度重建误差

Table 2　2D temperature reconstruction error at different noise intensity obtained based on WMS and DAS

Noise level / (dB · Hz^{-1})	WMS		DAS	
	D_e	E_m/K	D_e	E_m/K
−140	0.0206	49.8	0.0795	353.6
−150	0.0193	45.6	0.0359	155.9
−160	0.0192	41.6	0.0217	71.3
Non-noise	0.0186	40.3	0.0192	42.5

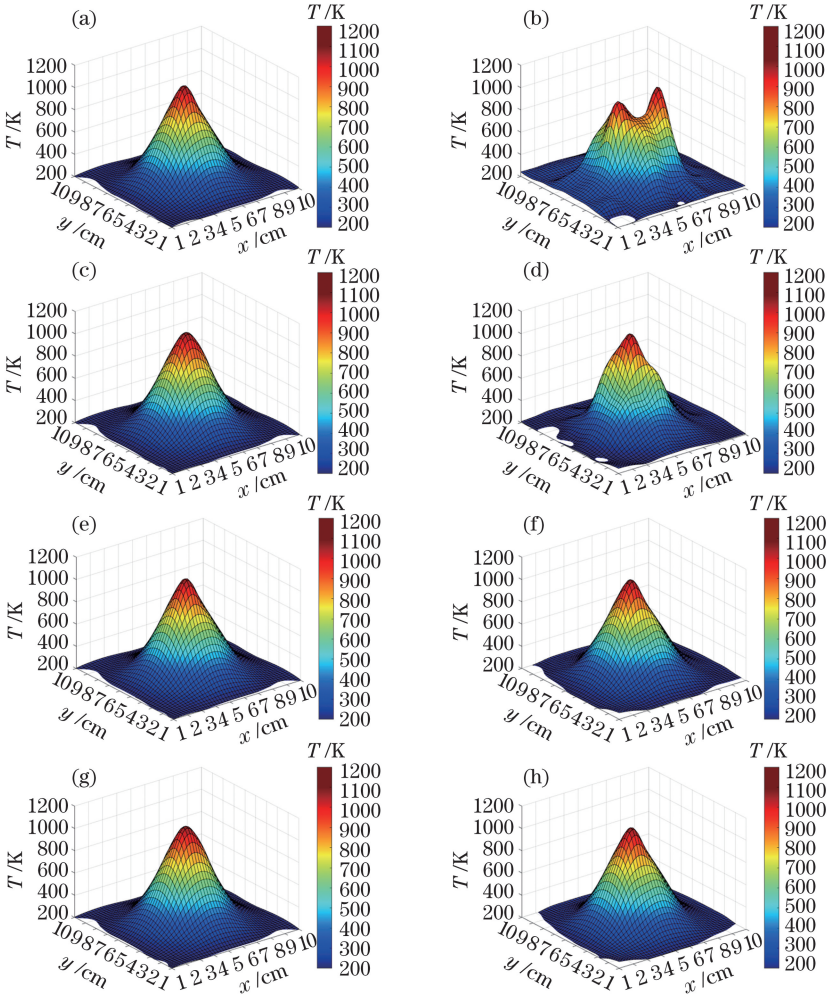

图 3　不同噪声强度下的重建结果。(a)在 I_{RIN} = −140 dB · Hz^{-1} 下基于 WMS 的重建结果；(b)在 I_{RIN} = −140 dB · Hz^{-1} 下基于 DAS 的重建结果；(c)在 I_{RIN} = −150 dB · Hz^{-1} 下基于 WMS 的重建结果；(d)在 I_{RIN} = −150 dB · Hz^{-1} 下基于 DAS 的重建结果；(e)在 I_{RIN} = −160 dB · Hz^{-1} 下基于 WMS 的重建结果；(f)在 I_{RIN} = −160 dB · Hz^{-1} 下基于 DAS 的重建结果；(g)未加噪声条件下基于 WMS 的重建结果；(h)未加噪声条件下基于 DAS 的重建结果

Fig. 3　Reconstruction results under different noise intensity. (a) Result obtained based on WMS for I_{RIN} = −140 dB · Hz^{-1}; (b) result obtained based on DAS for I_{RIN} = −140 dB · Hz^{-1}; (c) result obtained based on WMS for I_{RIN} = −150 dB · Hz^{-1}; (d) result obtained based on DAS for I_{RIN} = −150 dB · Hz^{-1}; (e) result obtained based on WMS for I_{RIN} = −160 dB · Hz^{-1}; (f) result obtained based on DAS for I_{RIN} = −160 dB · Hz^{-1}; (g) result obtained based on WMS without noise; (h) result obtained based on DAS without noise

这一结果表明在存在测量噪声时，基于 WMS 的重建方法的重建精度高于基于 DAS 的重建方法，基于 WMS 的重建方法对噪声的抑制作用在二维重建中仍然有效。在弱吸收流场条件下，基于 WMS 的重建方法能有效抑制测量中的噪声影响，显示出比基于 DAS 的重建方法更高的测量精度。

4　二维燃烧流场实验

4.1　实验系统设计

为了证明上述仿真的有效性，本文通对真实燃烧流场的温度重建，来进一步说明基于 WMS 的二维重建技术的重建结果优于基于 DAS 的二维重建技术。实验采用 McKenna 标准平焰炉产生的稳态火焰作为测量对象。实验所采用的测量系统如图 4 所示，实验中通过音速喷嘴控制甲烷与压缩空气的流量，甲烷与空气在管路中混合，在平焰炉表面被点燃。

基于时分复用技术，1395 nm 激光器与 1392 nm 激光器通过 2×12 光纤分束器连接到自制的准直器夹具上，待测流场被划分成 17 个大小不一的网格，如图 5 所示。射线布置方式如图 6 所示，测量位置位于 McKenna 平焰炉上方 30 mm 处的平面（激光束到 McKenna 平焰炉表面的距离 H = 30 mm），任一网格内至少有 4 条射线穿过。

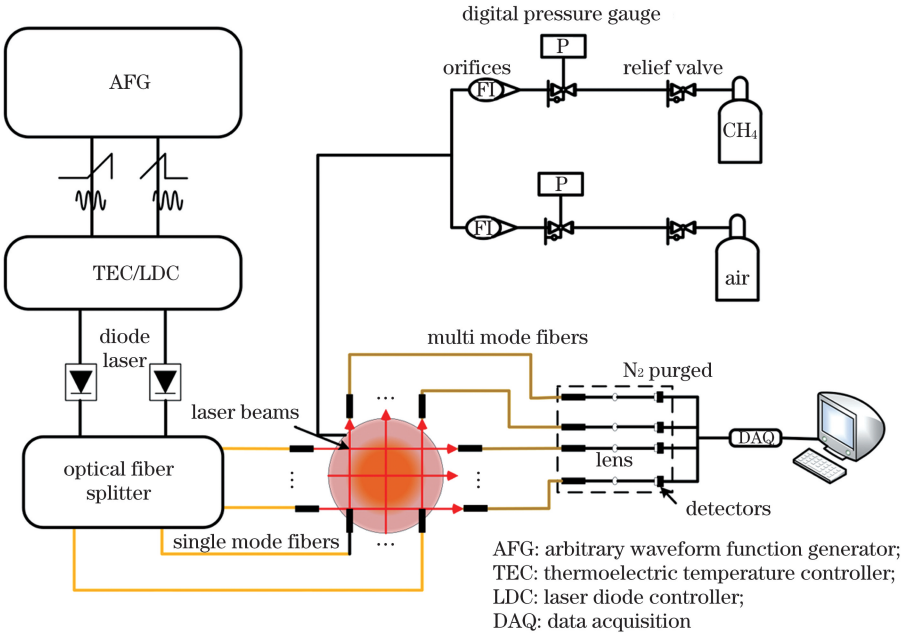

图 4　测量系统原理图

Fig. 4　Schematic diagram of measurement system

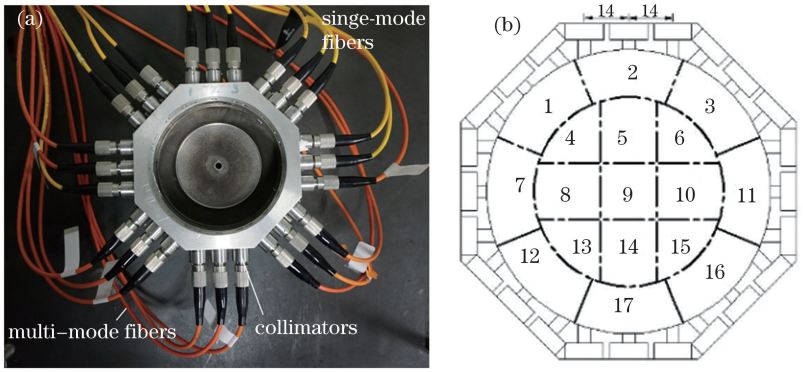

图 5　准直器安装夹具模型和待测流场网格划分示意图。(a)准直器安装夹具模型；(b)待测流场网格划分示意图

Fig. 5　Model of collimator installation fixture, and grid division diagram of flow field to be tested. (a) Model of collimator installation fixture; (b) grid division diagram of flow field to be tested

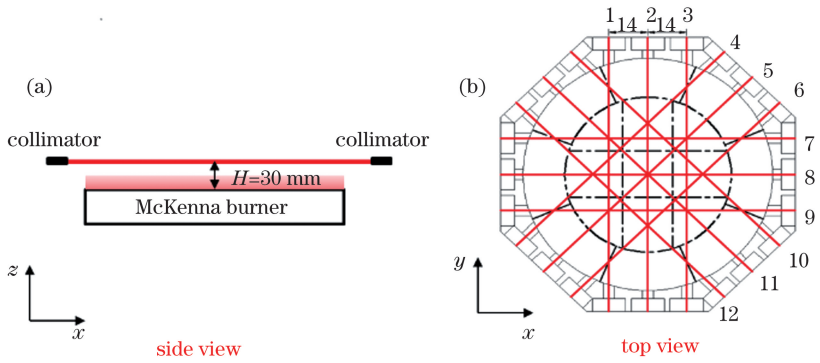

图 6 射线布置及位置测量示意图。(a)射线布置;(b)位置测量

Fig. 6 Schematic diagram of ray arrangement and position measurement. (a) Ray arrangement; (b) position measurement

4.2 测量结果

对于上述燃烧流场,利用热电偶对燃烧流场的温度进行标定测量。图 7(a)是利用热电偶在各网格内测得的结果,图 7(b)是经过线性插值处理得到的温度分布结果。

待测流场温度分布呈中间温度高、边缘温度低的特点,流场温度范围为 463~663 K。在区域 A(中心到 50 mm 直径范围)外,温度从燃烧炉边缘的 463 K 逐渐上升至最高温度 663 K。在区域 A 内,温度分布一致,均为 663 K。

在基于 DAS 的二维温度测量中,两个激光器基于时分复用方式将输出激光分成 12 路耦合激光,12 路激光按图 6 方式穿过待测流场,利用 12 路探测器接收 12 路直接吸收光谱信号。利用获得的 12 条吸收谱线信号,使用 MAART 算法进行反演重建,得到燃烧场温度分布结果如图 8(a)所示。

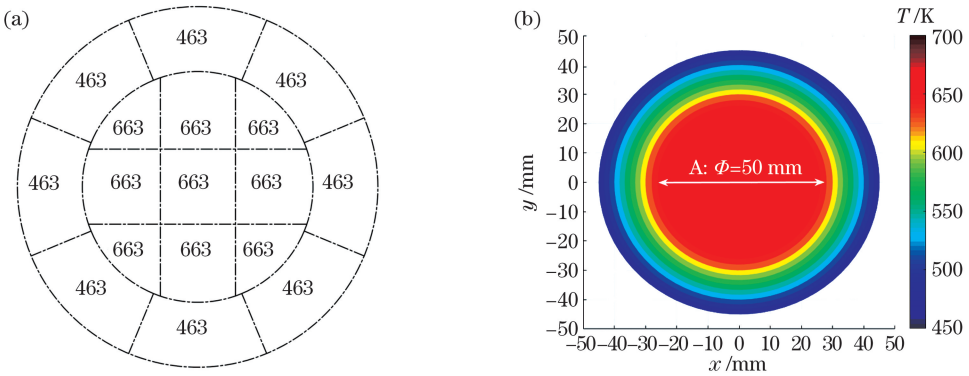

图 7 热电偶测量得到的流场温度分布(单位:K)。(a)插值前;(b)插值后

Fig. 7 Temperature distributions of flow field measured by thermocouple (units: K). (a) Before interpolation; (b) after interpolation

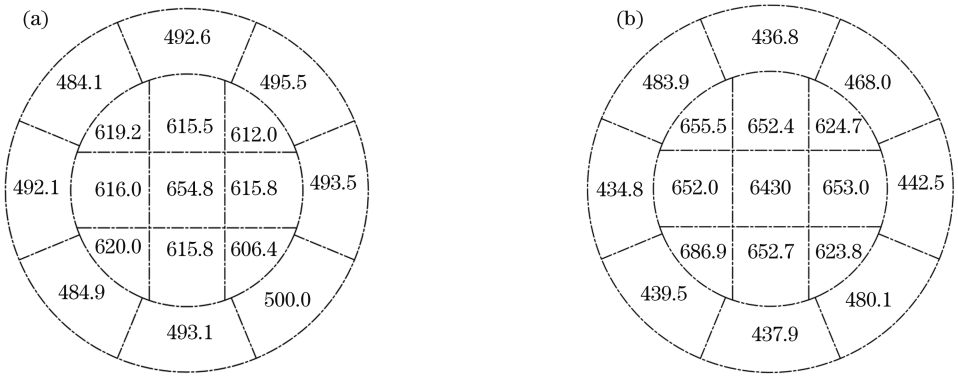

图 8 温度重建结果(单位:K)。(a) 基于 DAS 的重建方法 ;(b) 基于 WMS 的重建方法

Fig. 8 Results of temperature reconstruction (units: K). (a) Reconstruction method based on DAS; (b) reconstruction method based on WMS

重建温度场与热电偶测量结果之间的最大偏差出现在区域 A 边缘处，约为 56.6 K(8.5%)，重建温度场的均方相对误差为 0.0469。可以看出，基于 DAS 的温度重建结果虽然基本反映出燃烧流场的温度分布特点，但整体误差偏大。这种误差主要来源于噪声引起的基线拟合误差与 Voigt 线型拟合误差，而在弱吸收环境下，基线拟合误差造成的影响更为严重。对于二维重建，射线的线型拟合误差将影响代数迭代重建(ART)的二维重构精度，最终表现为温度重建误差。选择吸收更强时的吸收谱线将有助于减小 DAS 方法在二维重建中的误差。

基于 WMS 的二维温度测量与基于 DAS 的二维温度测量实验步骤不同的是，实验中的激光信号为叠加了高频调制信号的锯齿波信号。使用 WMS 光谱处理方法获得 12 路光路 $S_{2f/1f}$ 信号，使用 MAART 算法对上述投影信号进行重建，求得流场温度二维分布。使用基于 WMS 的方法获得的燃烧流场温度二维分布结果如图 8(b)所示。计算得到重建温度场最大偏差为 39.2 K，同样区域 A 边缘处，最大偏差对应的相对误差为 5.9%，均方相对误差为 0.0268。总体来说，基于 WMS 的重建技术的重建结果与热电偶测量结果基本一致，测量结果误差优于基于 DAS 的重建技术结果。在一维 TDLAS 中，WMS 方法不受基线上噪声的影响，并且对吸收峰处的噪声有明显的抑制作用，这一点也体现在基于 WMS 的二维重建中。由于经过调制与解调后的 $2f/1f$ 信号对环境噪声有较好的抑制作用，每一条射线信号具有较高的信噪比，而高信噪比的网格投影信号有助于更精确的二维重建。

4.3　分析与讨论

通过对得到的 17 个网格温度测量结果进行线性插值，得到了图 9 所示的插值后的二维温度场测量结果及其偏差。

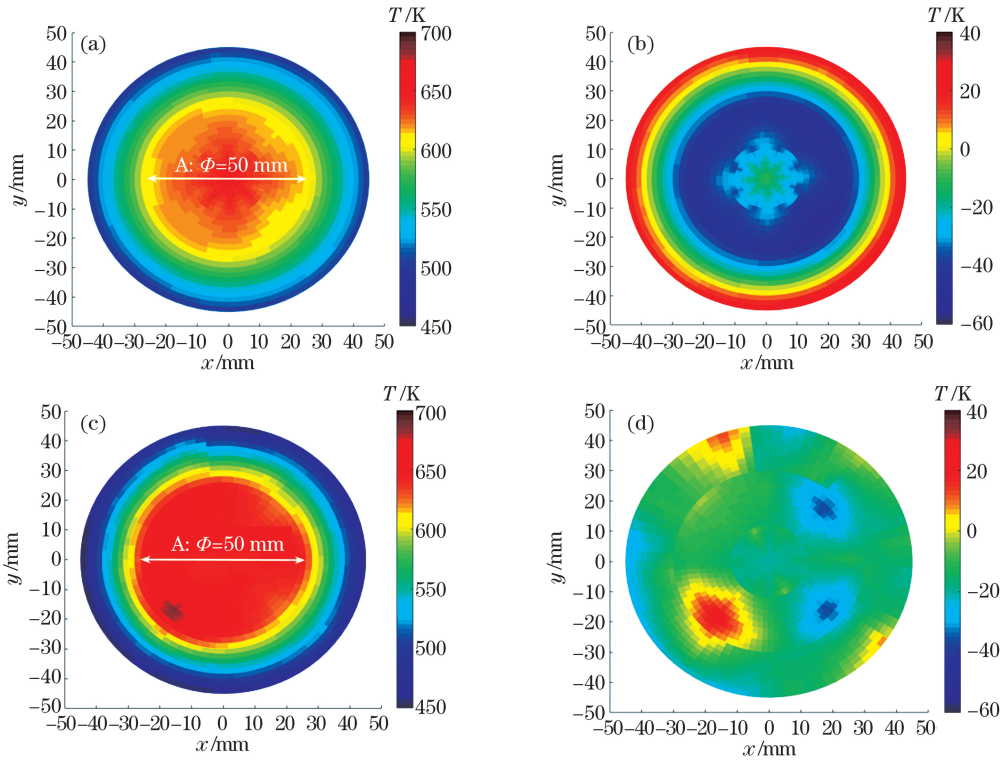

图 9　温度重建结果和温度测量偏差。(a)基于 DAS 的温度重建结果；(b)基于 DAS 的温度测量偏差；(c)基于 WMS 的温度重建结果；(d)基于 WMS 的温度测量偏差

Fig. 9　Results of temperature reconstruction and deviation of temperature measurement. (a) Result of temperature reconstruction based on DAS; (b) deviation of temperature measurement based on DAS; (c) result of temperature reconstruction based on WMS; (d) deviation of temperature measurement based on WMS

采用基于 DAS 的重建方法得到的温度分布重建结果总体呈现中间温度高、边缘温度低的特点，温度呈中心对称分布，如图 9(a)所示。在区域 A 外，温度分布与热电偶测量结果一致，即由边缘的 490 K 逐渐增加至中心的 606 K，温度值略低于热电偶测量结果。在区域 A 内，温度重建结果并未呈

现出平稳分布特点，重建结果为由边缘向中心逐渐增加。中心位置的温度为重建温度场的最高值，即650 K，同样略低于热电偶测量结果。重建偏差分布在－54.5～33.2 K之间，整体偏大。

如图9(c)所示，采用基于WMS的重建方法测量得到的温度场重建结果同样呈现中间温度高、边缘温度低的特点，基本上呈中心对称分布，且与热电偶测量结果吻合较好。在区域A外，温度分布与热电偶测量结果一致，即温度由边缘向中心逐渐增加。在这一范围内，边缘温度约为450 K，然后逐渐增加至651 K，重建温度略低于热电偶测量结果。在区域A内，温度重建结果呈现出较为平稳的分布特点，与热电偶测量结果较为一致。重建偏差分布在－34.3～22.8 K之间，较基于DAS的重建方法的重建结果小，且整体偏差较小。

通过对比基于DAS与WMS的两种重建方法的重建结果，可以看出基于WMS的二维重建方法有更高的重建精度，且整体偏差较小，这应该得益于基于WMS的二维重建方法有效抑制了系统的低频噪声，提高了原始测量信号的信噪比，从而使得在弱吸收环境下获得的测量效果优于基于DAS的二维重建方法的重建结果。

研究结果表明，相比于基于DAS的二维重建方法，基于WMS的二维重建方法更适用于在噪声影响较大环境下的二维流场重建，如超燃冲压发动机燃烧室内的流场二维重建、高超声速风洞流场质量评估。

5 结　论

将WMS方法与ART相结合的方法应用于燃烧流场二维重建，该方法的重建速度快，所需谱线数量少，在实际应用中具有较大的优势。从数值模拟与实验验证两方面分析了基于DAS的二维重建与基于WMS的二维重建之间的差异，论证了在一维TDLAS中，WMS较DAS对噪声具有更好的抑制作用这一特点，得到WMS仍然适用于二维重建的结论。

在数值模拟中，分析了不同噪声水平下的两种方法的重建结果的差异，结果显示随着噪声水平的增加，基于WMS的二维重建有更好的鲁棒性，而基于DAS的二维重建受噪声影响比较明显。在较大噪声水平情况下，基于DAS的二维重建方法的重建结果不能准确反映模拟流场环境的特点。在实验验证中，搭建了平面燃烧流场二维重建测量实验系统，选择了两条常用的水蒸汽吸收谱线7168.44 cm^{-1}与7185.60 cm^{-1}。采用基于DAS和WMS的两种重建方法，对燃烧流场的温度分布进行了二维重建测量。将采用基于DAS和WMS的两种重建方法得到的重建结果与热电偶测得的结果进行对比，发现最大偏差分别为8.5%、5.9%，均方相对误差分别为0.0469、0.0268。结果显示了基于WMS的二维重建有着比基于DAS的二维重建更好的抗噪声能力，这表明弱吸收下基于WMS的二维重建方法的重建精度优于基于DAS的二维重建方法。

研究结果表明，基于WMS的二维重建方法适用于如超燃冲压发动机燃烧室内的流场二维重建、高超声速风洞流场质量评估等噪声影响较大的工程应用。

参　考　文　献

[1] Liu C, Xu L J. Laser absorption spectroscopy for combustion diagnosis in reactive flows: a review[J]. Applied Spectroscopy Reviews, 2019, 54(1): 1-44.

[2] Liu C, Xu L J, Cao Z, et al. Measurement of nonuniform temperature and concentration distributions by combining line-of-sight tunable diode laser absorption spectroscopy with regularization methods [J]. Applied Optics, 2013, 52(20): 4827-4842.

[3] Fomin A, Sharabi Y, Pilipodi Best A, et al. Concentration measurements by intracavity laser absorption spectroscopy for the case of strongly overlapped spectra [J]. Applied Physics B, 2018, 124: 164.

[4] Qu Q W, Cao Z, Xu L J, et al. Reconstruction of two-dimensional velocity distribution in scramjet by laser absorption spectroscopy tomography [J]. Applied Optics, 2019, 58(1): 205-212.

[5] Murzyn C, Sims A, Krier H, et al. High speed temperature, pressure, and water vapor concentration measurement in explosive fireballs using tunable diode laser absorption spectroscopy [J]. Optics and Lasers in Engineering, 2018, 110: 186-192.

[6] Xu L, Liu C, Jing W, et al. Tunable diode laser absorption spectroscopy-based tomography system for on-line monitoring of two-dimensional distributions of temperature and H_2O mole fraction [J]. The Review of Scientific Instruments, 2016, 87(1): 013101.

[7] Zhang Z R, Sun P S, Pang T, et al. Reconstruction of combustion temperature and gas concentration distributions using line-of-sight tunable diode laser absorption spectroscopy [J]. Optical Engineering.

2016, 55(7): 076107.

[8] Jeon M G, Deguchi Y, Kamimoto T, et al. Performances of new reconstruction algorithms for CT-TDLAS (computer tomography-tunable diode laser absorption spectroscopy)[J]. Applied Thermal Engineering, 2017, 115: 1148-1160.

[9] Liu X, Zhang G, Huang Y, et al. Two-dimensional temperature and carbon dioxide concentration profiles in atmospheric laminar diffusion flames measured by mid-infrared direct absorption spectroscopy at 4.2 μm [J]. Applied Physics B: Lasers & Optics, 2018, 124(4): 61-71.

[10] Jeon M G, Doh D H, Deguchi Y, et al. Evaluation of 3D measurement using CT-TDLAS [J]. Modern Physics Letters B, 2019, 33(14n15): 1940018.

[11] Emmerman P J, Goulard R, Santoro R J. Multiangular absorption diagnostics of a turbulent argon-methane[J]. Journal of Energy, 1980, 4(2): 70-77.

[12] Gorenflo R, Vessella S. Abel integeral-equations-analysis and applocations [J]. Lecture Notes In Mathematics, 1991, 1461: 1-209.

[13] Ma L, Cai W W. Numerical investigation of hyperspectral tomography for simultaneous temperature and concentration imaging[J]. Applied Optics, 2008, 47(21): 3751-3759.

[14] Ling N, Wen C S. Modified adaptive algebraic tomographic reconstruction of gas distribution from incomplete projection by a two-wavelength absorption scheme[J]. Chinese Optics Letters, 2011, 9(6): 061201.

[15] Terzija N, Davidson J L, Garcia-Stewart C A, et al. Image optimization for chemical species tomography with an irregular and sparse beam array [J]. Measurement Science and Technology, 2008, 19(9): 094007.

[16] Jackson K, Gruber M, Buccellato S. HIFiRE flight 2 project overview and status update 2011[C]//17th AIAA International Space Planes and Hypersonic Systems and Technologies Conference, 11 April 2011-14 April 2011, San Francisco, California. Reston, Virginia: AIAA, 2011.

[17] Rieker G B, Jeffries J B, Hanson R K. Calibration-free wavelength-modulation spectroscopy for measurements of gas temperature and concentration in harsh environments[J]. Applied Optics, 2009, 48(29): 5546-5560.

[18] Silver J A, Kane D J, Greenberg P S. Quantitative species measurements in microgravity flames with near-IR diode lasers[J]. Applied Optics, 1995, 34(15): 2787-2801.

[19] Guha A, Schoegl I M. Tomographic imaging of flames: assessment of reconstruction error based on simulated results [J]. Journal of Propulsion and Power, 2014, 30(2): 350-359.

[20] Zhao W S, Xu L J, Huang A, et al. A WMS based TDLAS tomographic system for distribution retrievals of both gas concentration and temperature in dynamic flames[J]. IEEE Sensors Journal, 2020, 20(8): 4179-4188.

[21] Cai W W, Kaminski C F. Multiplexed absorption tomography with calibration-free wavelength modulation spectroscopy [J]. Applied Physics Letters, 2014, 104(15): 154106.

[22] Peng D. Research on the diagnosis of complex flow field using tunable diode laser absorption spectroscopy[D]. Hefei: University of Science and Technology of China, 2019: 89-96.
彭冬. 吸收光谱技术在复杂流场诊断中的应用研究[D]. 合肥: 中国科学技术大学, 2019: 89-96.

[23] Zhang B Q, Xu Z Y, Liu J G, et al. Absorption model of wavelength modulation spectroscopy in combustion flow field[J]. Chinese Journal of Lasers, 2019, 46(7): 0711001.
张步强, 许振宇, 刘建国, 等. 燃烧流场波长调制光谱吸收模型的研究[J]. 中国激光, 2019, 46(7): 0711001.

[24] Qu D S, Fan H J, Liu L W, et al. Measurement of gas parameters in supersonic combustion field based on near-infrared spectroscopy [J]. Acta Optica Sinica, 2020, 40(3): 0330001.
屈东胜, 樊宏杰, 刘连伟, 等. 基于近红外光谱的超声速燃烧场气体参数测量研究[J]. 光学学报, 2020, 40(3): 0330001.

[25] Yao D L, Chen S. Study on TDLAS measurement method for plume velocity of solid rocket motor[J]. Journal of Applied Optics, 2020, 41(2): 342-347.
姚德龙, 陈松. 固体火箭发动机羽流流速 TDLAS 测量方法研究[J]. 应用光学, 2020, 41(2): 342-347.

[26] Lins B, Zinn P, Engelbrecht R, et al. Simulation-based comparison of noise effects in wavelength modulation spectroscopy and direct absorption TDLAS[J]. Applied Physics B, 2010, 100(2): 367-376.

Two-Dimensional Reconstruction of Combustion Flow Field Using Wavelength-Modulated Absorption Spectra

Wang Xingping[1,2], Peng Dong[1], Li Jiasheng[1], Jin Yi[3*], Zhai Chao[3]

[1] *School of Engineering Science, University of Science and Technology of China, Hefei, Anhui 230027, China;*

[2] *Anhui Institute of Optics and Fine Mechanics, Chinese Academy of Science, Hefei, Anhui 230027, China;*

[3] *Experimental Center of Engineering and Material Science, University of Science and Technology of China, Hefei, Anhui 230027, China*

Abstract

Objective The measurement of key parameters of combustion flow field can effectively evaluate combustion efficiency, control pollution emission, and improve energy efficiency. Because of its obvious superior features such as high precision, noncontact measurement, and low cost, tunable diode laser absorption spectroscopy (TDLAS) is an effective way to measure temperature, concentration, velocity, and pressure in combustion flow field. Combined with computerized tomography (CT), TDLAS can achieve two-dimensional (2D) or three-dimensional (3D) tomography. In the 1980s, Emmerman et al. used the direct absorption spectroscopy (DAS) for combustion diagnosis in reactive flows, which verified the feasibility of the method to realize 2D combustion diagnosis. With the development of the laser and reconstruction algorithms, the DAS-based 2D reconstruction technology has begun to be applied to engineering practice. This technology has been successfully used in the Hypersonic International Flight Research Experiment (HIFiRE) conducted by the US Air Force Laboratory and NASA. Although the DAS exhibits many advantages, it is difficult to apply this method under low signal-to-noise ratio (SNR) conditions. The wavelength modulation spectroscopy developed on the basis of the DAS can significantly improve the SNR under weak absorption conditions, thus improving the detection accuracy and detection limit of the absorption spectroscopy. In line-of-sight measurement, the wavelength modulation spectroscopy (WMS) shows good noise resistance and is therefore suitable for the flow field measurement under weak absorption or high-pressure conditions. Calibration-free WMS (CF-WMS) proposed by Hanson′s group from Stanford University is one of the widely used WMS methods. As far as we know, the literature mainly focused on numerical simulation analysis for the difference in 2D reconstruction between the DAS and WMS. It is necessary to verify the difference between the two methods by experiment.

Methods Combined with the algebraic reconstruction technique (ART), we introduced the principle of two-dimensional temperature reconstruction based on WMS, and analyzed the difference between DAS and WMS in the two-dimensional reconstruction under the influence of various noises through numerical simulation. Next, the combustion flow field generated by the McKenna flat flame furnace was used as the measurement object. The two-dimensional temperature measurement experimental system was built around the flat flame furnace. DAS- and WMS-based two-dimensional temperature reconstructions of methane-air premixed flame with an equivalent ratio of 1 were carried out, and the reconstruction results were analyzed.

Results and Discussions In numerical simulation, the temperature reconstruction results of the simulated flow field with two reconstruction methods under various noise intensities are provided (Table 2). The maximum deviation and mean square relative error of WMS are 0.0186 and 40.3 K, respectively, and those of DAS reconstruction are 0.0192 and 42.5 K, respectively. Under the condition of no noise, these values are relatively consistent. With the increase in noise intensity, the reconstruction error based on DAS gradually increases, while that of WMS does not change significantly. The maximum deviation and mean square relative error of WMS based reconstruction are 0.0206 and 49.8 K, respectively, and those of DAS based reconstruction are 0.0795 and 353.6 K, respectively (Fig. 3). Under the condition of noise intensity $I_{\mathrm{RIN}} = -140$ dB/Hz, these values are greatly different. This result shows that the reconstruction accuracy of the WMS based method is higher than that of the DAS based method in the presence of measurement noise, and the suppression effect of the WMS based method on noise is still effective in a two-dimensional reconstruction. Under the condition of a weak-absorption flow field, the two-dimensional reconstruction method based on the WMS can effectively suppress the influence of noise in measurement with higher measurement accuracy.

In experimental verification, the maximum deviation between the reconstructed temperature field obtained by

the DAS-based method and the thermocouple measurement result appeared in the range of 50 mm in diameter is about 56.6 K (8.5%), and the relative error of the mean square of the reconstructed temperature field is 0.0469 (Fig. 9). Although the reconstruction results based on DAS reflect the temperature distribution characteristics of the combustion flow field, the overall error is relatively large. This error mainly comes from the baseline fitting error and the Voigt fitting error caused by noise, while the influence of the baseline fitting error is more serious in a weak absorption environment. For a 2D reconstruction, the Voigt fitting error will affect the accuracy of ART 2D reconstruction, and it will eventually show up as a temperature reconstruction error. Selecting absorption spectral lines with stronger absorption will help reduce the error of the DAS based method in a two-dimensional reconstruction. The maximum deviation of the reconstructed temperature field obtained by the WMS-based method is 39.2 K (5.9%), which also occurred in the range of 50 mm in diameter (Fig. 9). The relative error of mean square is 0.0268. In general, the reconstruction result based on WMS is consistent with the thermocouple measurement result, and the measurement error is smaller than that of the DAS-based method. In one-dimensional TDLAS, WMS is not affected by the baseline and has significant inhibition effect on the noise at absorption peak, which is also reflected in 2D reconstruction. As the $2f/1f$ signal has a better suppression effect on the environmental noise, the signal of each ray has a higher SNR, which is helpful to a more accurate 2D reconstruction.

Conclusions In this paper, WMS combined with ART is applied to the two-dimensional reconstruction of the combustion flow field. The reconstruction speed is large, and the number of spectral lines required is small, which has great advantages in practical applications. From the numerical simulation and experimental verification, the difference between DAS- and WMS-based 2D reconstruction is analyzed. It is proved that WMS has a better suppression effect on noise than DAS in a 2D TDLAS. In a numerical simulation, the difference in the reconstruction result between the two methods under different noise levels is analyzed. The result shows that with the increase in the noise level, a WMS-based 2D reconstruction has better robustness while a DAS-based 2D reconstruction varies significantly. In the case of a high noise level, a DAS-based 2D reconstruction cannot accurately reflect the characteristics of a simulated flow field environment. In an experimental verification, by comparing with the result measured by the thermocouple, we find that the maximum deviations of the DAS-based 2D reconstruction and WMS-based 2D reconstruction are 8.5% and 5.9%, respectively, and the mean square relative errors are 0.0469 and 0.0268, respectively. The results show that the WMS-based 2D reconstruction has higher anti-noise capability than DAS-based 2D reconstruction and the accuracy of a WMS-based 2D reconstruction is higher than that of the DAS-based 2D reconstruction under weak absorption. It is advised that a WMS-based two-dimensional reconstruction method is suitable for engineering applications where noise has a great impact, such as 2D reconstruction of flow field in a scramjet combustion chamber and the wind tunnel flow field quality assessment.

Key words laser technique; spectroscopy; wavelength modulation spectroscopy; two-dimensional reconstruction; combustion diagnosis

OCIS codes 140.3600; 300.1030; 300.6260; 300.6340